Influences of the boundary layer evolution on surface ozone variations at a tropical rural site in India

K K Reddy[1], M Naja[2,4,*], N Ojha[2,4], P Mahesh[1] and S Lal[3]

[1] *Yogi Vemana University, Kadapa, Tirupati, India.*
[2] *Aryabhatta Research Institute of Observational Sciences, Manora Peak, Nainital 263 129, India.*
[3] *Physical Research Laboratory, Ahmedabad, Navrangpura 380 009, India.*
[4] *Department of Physics, Kumaun University, Nainital 263 001, India.*
[*] *Corresponding author. e-mail: manish@aries.res.in*

Collocated measurements of the boundary layer evolution and surface ozone, made for the first time at a tropical rural site (Gadanki 13.5°N, 79.2°E, 375 m amsl) in India, are presented here. The boundary layer related observations were made utilizing a lower atmospheric wind profiler and surface ozone observations were made using a UV analyzer simultaneously in April month. Daytime average boundary layer height varied from 1.5 km (on a rainy day) to a maximum of 2.5 km (on a sunny day). Correlated day-to-day variability in the daytime boundary layer height and ozone mixing ratios is observed. Days of higher ozone mixing ratios are associated with the higher boundary layer height and *vice versa*. It is shown that higher height of the boundary layer can lead to the mixing of near surface air with the ozone rich air aloft, resulting in the observed enhancements in surface ozone. A chemical box model simulation indicates about 17% reduction in the daytime ozone levels during the conditions of suppressed PBL in comparison with those of higher PBL conditions. On a few occasions, substantially elevated ozone levels (as high as 90 ppbv) were observed during late evening hours, when photochemistry is not intense. These events are shown to be due to southwesterly wind with uplifting and northeasterly winds with downward motions bringing ozone rich air from nearby urban centers. This was further corroborated by backward trajectory simulations.

1. Introduction

The meteorological processes within the boundary layer strongly influence the dispersion, transport and chemistry of different air pollutants. The height of the convective boundary layer (CBL) is the most relevant parameter to study the air pollution events in detail, since it determines the volume of the atmosphere into which various pollutants and their precursors are mixed. The role of the CBL can be more pronounced over the tropical region, whereby virtue of its location, convection is stronger in comparison with other parts of the world. Different aspects of the complex structure and dynamics of the boundary layer are not well understood over the tropical Indian region and hence there are not much extensive studies in the pollution dispersion modelling and meteorological now-casting over this region where the dynamics of the CBL plays an important role. Diurnal variation in the boundary layer height has significant contribution in deciding the air-quality standard during

Keywords. Wind profiler; boundary layer; surface ozone; box model; air trajectory; atmospheric sciences; instruments and techniques/experiments; modelling.

different times of the day. Therefore it is necessary to have simultaneous observations of trace species and the boundary layer evolution to study these aspects.

To study the boundary layer dynamics over the Indian region, few attempts were made using the acoustic sounders, towers and radiosonde (Singal *et al.* 1982; Ramachandran *et al.* 1994; Reddy *et al.* 1995). However, Sodars and towers work well only for lower boundary layer heights, while radiosonde data suffer from coarse spatial and temporal resolution. Lower atmospheric wind profilers (LAWP) have been found very suitable for the observations of the CBL dynamics with better spatial and temporal coverage (e.g., Reddy *et al.* 2002; Krishnan *et al.* 2003; Rao and Rao 2007).

Ozone in the boundary layer is considered as one of the criteria pollutants due to its adverse effects on the living beings and vegetation. It also plays a key role in the atmospheric chemistry and climate change. The major source of the tropospheric ozone is *in situ* photo-oxidation of some of the pollutants including CO, methane and other hydrocarbons in presence of sufficient amount of NO_x. Downward transport of ozone rich air from the stratosphere is the other source of the tropospheric ozone. Out of these two sources, *in situ* photochemistry is shown to have dominant contribution particularly in the boundary layer (e.g., Crutzen 1995). This ozone pollution was once thought to be restricted to the urban areas only but now it is well accepted that ozone levels in the rural areas can rival those measured in urban areas. Ozone and precursors can get transported from urban regions to the rural areas, thus it is very important to understand the role of chemistry and dynamics for controlling ozone pollution in the rural areas.

Notably, ozone production efficiency is very much different (lower) over south Asia, as compared to N. America or Europe (Naja and Lal 2002), i.e., even the levels of precursor gases are higher over south Asia but not the ozone levels (Lelieveld *et al.* 2001). Simultaneous occurrence of biomass burning and fossil fuel emissions in the same airmasses over the south Asia make very different situation here in comparison with the other parts of the world (Reiner *et al.* 2001). This also makes this region important to study the influence of the boundary layer process on surface ozone in such a different chemical environment. It is now well recognized that CBL processes like entrainment and fumigation can significantly alter the vertical distribution of ozone and related precursors near the surface (Zhang and Rao 1999; Rao *et al.* 2003). Further, the production of OH is highest over the tropical regions due to the availability of intense solar radiation and large water vapour content (80% of the global budget). This feature makes the tropical region photochemically most active (e.g., Crutzen 1995). Brasseur *et al.* (1998) showed that the change in tropical ozone is highly sensitive to climate forcing in the tropics.

Considering the importance of tropical troposphere, attempts have been made for the measurement of ozone and precursors along with meteorological parameters over the Indian region in which the roles of chemistry and meteorology in controlling the ozone levels have been examined over this region (e.g., Naja and Lal 1997; Lal *et al.* 2000; Naja *et al.* 2003; David and Nair 2011). However, over the Indian region, so far simultaneous observations of ozone and BL are not reported. Here, we have utilized the simultaneously available one month data of ozone and the boundary layer over a tropical rural site in the southern part of India and the role of the boundary layer dynamics are discussed in the ozone variations.

2. Observation site and measurement techniques

The observation site, Gadanki (13.5°N, 79.2°E, 375 m above mean sea level), is about 30 km from Tirupati city in the southern part of India (figure 1). There are hills in the northern and southern sides of the observation site within 1 to 10 km distance and the average height of the hills is about 750 m, with a maximum height of about 1300 m (e.g., Reddy *et al.* 2002). A major road passes near the observation site, with the usage of a few thousands of vehicles each day. The population of Gadanki is about 1000 only, while that of Tirupati is about 0.5 million. There are no major industries nearby except few small-scale units at Tirupati. The observation site is about 120 and 150 km from the two nearby major cities, Chennai (Madras) to the southeast and Bangalore to the southwest, respectively (figure 1). Simultaneous observations of both LAWP and ozone are available for April and for a few days in May 1999. Here we have used one full month data of April 1999 only.

2.1 *Lower atmospheric wind profiler (LAWP)*

The lower atmospheric wind profiler operates at a frequency of 1357.5 MHz with a beam width of 4° oriented in the north, east and zenith directions at 15.5° zenith angle. It is capable of measuring the three dimensional wind vector from ∼300 m to about 4000 m with a 150 m resolution in the vertical and with a precision of 1 m/s for the wind speed and 1 degree for the wind direction. Further details of LAWP setup at Gadanki can be seen in Reddy *et al.* (2002). Gadanki LAWP is operated

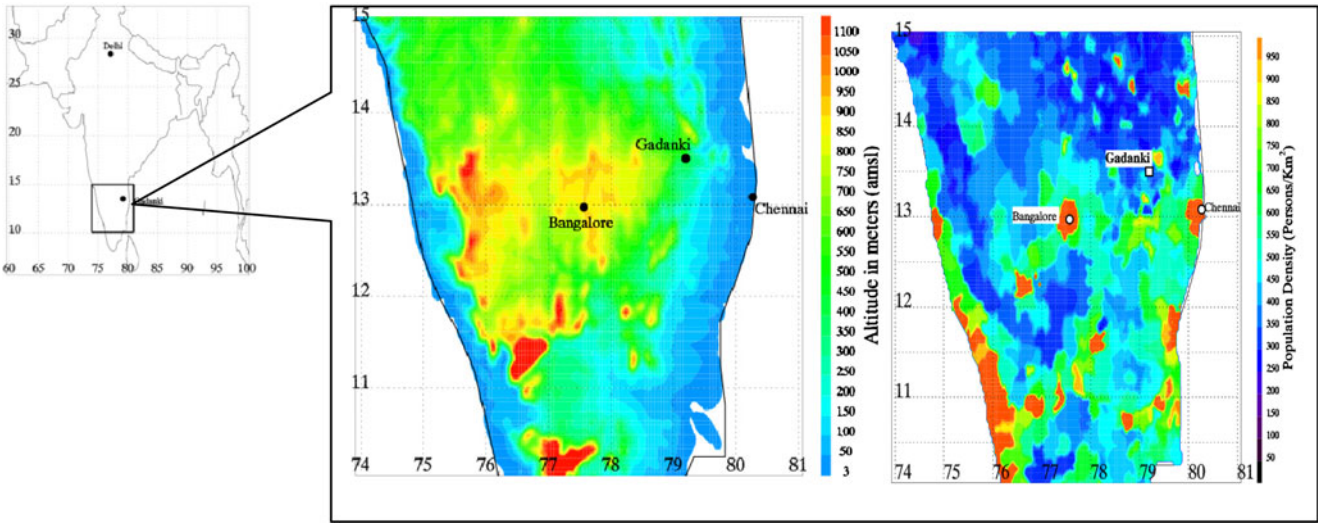

Figure 1. Map showing the geographical location of the observation site in India along with the information on the topography and population density around the site.

Table 1. *Specifications of lower atmospheric wind profiler (LAWP) at Gadanki.*

Parameter		Specification	
Frequency	:	1357.5 MHz	
Maximum bandwidth	:	2 MHz	
Peak power	:	1 kW	
Maximum duty ratio	:	5%	
Antenna type	:	Phased arrays	
Antenna aperture	:	3.8×3.8 m^2	
Beamwidth	:	4°	
		Low mode	High mode
Pulse width	:	1 μs	2 μs
Inter pulse period	:	60 μs	80 μs
Sampling interval	:	1 μs	1 μs
Start height	:	150 m	150 m
Number of coherent integrations	:	70	50
Number of incoherent integrations	:	100	64
Number of FFT points	:	128	128
Number of beam	:	3 beams (15.5° off zenith of north and east and vertical)	

in two modes, low and high mode, alternatively with a range resolution of 150 m (as shown in table 1). The CBL height is deduced from the range corrected signal-to-noise ratio (SNR) recorded by this wind profiler. The technique is based on experimental and theoretical evidence indicating that the profile of structure intensity parameter, C_n^2, exhibits a peak at the inversion, capping the mixed layer (Wyngaard and LeMone 1980; Fairall 1991). The wind profiler SNR at a given range is directly proportional to C_n^2 (VanZandt *et al.* 1978). Mixing-height and CBL-wind data are available every 5 min and are averaged over 1 hr. Each 1 hr mixing-height data point represents a median over 12 measurements. Because range gates were at 150 m intervals, the hourly data thus represent the true median mixing-height ± 75 m. Uncertainty in the CBL wind data is about 1 m/s (Reddy *et al.* 2002).

2.2 *Ozone analyzer*

Ozone measurements were made using an online ozone analyzer (Environment S.A., France; Model

O3 41M) based on the well known technique of UV light (253.7 nm) absorption by ozone molecules. The analyzer incorporates corrections due to changes in temperature and pressure in the absorption cell and drift in the intensity of UV lamp. The absolute accuracy of these UV absorption based analyzers is reported to be about 5% (Kleinman *et al.* 1994). The minimum detection limit of the analyzer is about 1 ppbv and its response time is about 10 s. Average data was collected at 15 minutes interval. This analyzer has an in built ozone generator for the calibration and a procedure for zero corrections. More descriptions of the system used in this study including its calibration, zero checking, maintenance and other details can be seen in Naja and Lal (2002).

2.3 *Chemical box model simulations*

NCAR-Master Mechanism (NCARMM), a chemical box model (zero dimension), developed at National Center for Atmospheric Research, USA, has been used here. This model consists of explicit and highly detailed gas phase chemical mechanism with a box model solver (http://cprm.acd.ucar.edu/Models/MasterMech/). User inputs are species of interest, emissions, initial and background concentrations, variations in boundary layer height and dilution rates. Tropospheric Ultraviolet and Visible (TUV) radiation model, included in the code package, is used to estimate the photolysis rates. Further details of this model can be seen in the Madronich (2006) and Madronich and Flocke (1999). The present model setup has been initiated with O_3, H_2O, NO, NO_2, CO, OH, HO_2, CH_2O, CH_4, *i*-butane, *n*-butane, Isoprene, Xylene, and Toluene while N_2, O_2, M and photons are hard-wired in this model.

2.4 *Backward trajectory simulation*

Influences of different airmasses are studied using backward trajectories at Gadanki using Hybrid Single-Particle Lagrangian Integrated Trajectory (HYSPLIT) Model (http://ready.arl.noaa.gov/HYSPLIT.php). HYSPLIT model is driven by meteorological fields from NCEP reanalysis dataset available every 6 hours at a spatial resolution of 2.5°. Five days backward trajectories at three altitude levels (500, 1000 and 1500 m agl) are simulated. Isentropic method has been chosen for the vertical motion calculations in this study. Further details about trajectory simulations using HYSPLIT model can be seen elsewhere (Draxler and Rolph 2011; Rolph 2011).

3. Results

3.1 *Diurnal variation in ozone*

Figure 2 shows the box plot of average diurnal variation in surface ozone at Gadanki during April. Daytime higher ozone levels are mainly due to the photochemical production of ozone (Naja and Lal 2002). Lower ozone mixing ratios during the night-time are mainly due to ozone titration by NO in the shallower boundary layer along with the depositional losses. Apart from the role of photochemistry, boundary layer meteorology and dynamics also play a key role in ozone variability (e.g., Banta *et al.* 1998; White *et al.* 2002). Boundary layer starts evolving gradually after the sunrise and attains the maximum height during afternoon hours due to the increase in surface heating. During this time, trace species gets vigorously mixed with in, thus forming convective mixed layer. Through this mixing of the air, from lower altitudes with that of aloft, ozone distribution near the surface and above it is significantly altered. The impact of the boundary layer processes on surface ozone at the present tropical rural site is discussed in the next section.

3.2 *Evolution of ozone and the convective boundary layer*

Day-to-day variations along with the diurnal variations in ozone from 1 April to 30 April clearly shows that there are large diurnal as well as day-to-day variability in the ozone levels at Gadanki (figure 3). Interestingly, there have been events

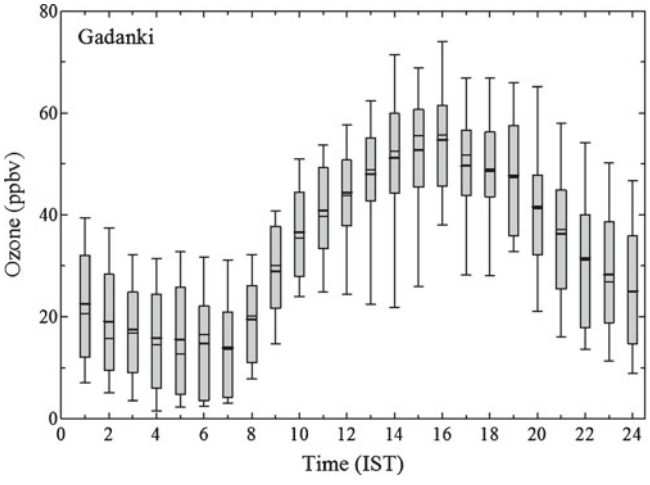

Figure 2. Monthly average ozone diurnal variations during April at Gadanki. Upper and lower sides of box are 75th and 25th percentile and whiskers are 95th and 5th percentiles. Thick and thin lines in the box are mean and median, respectively.

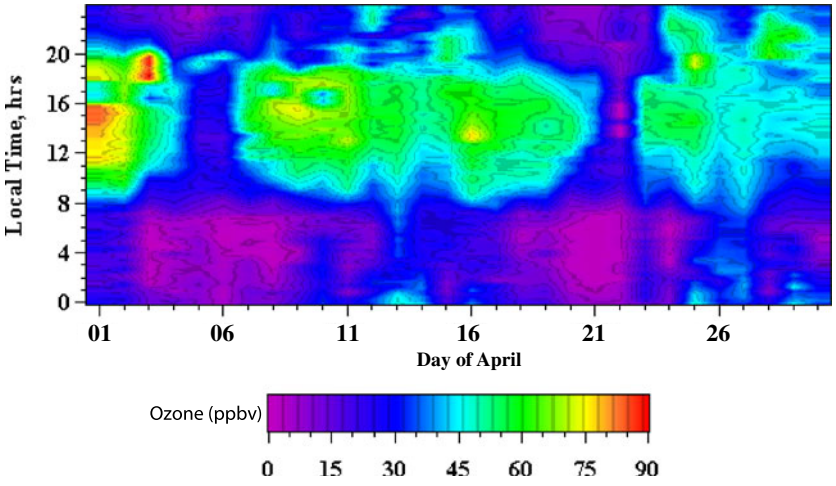

Figure 3. Diurnal and day-to-day variations in ozone.

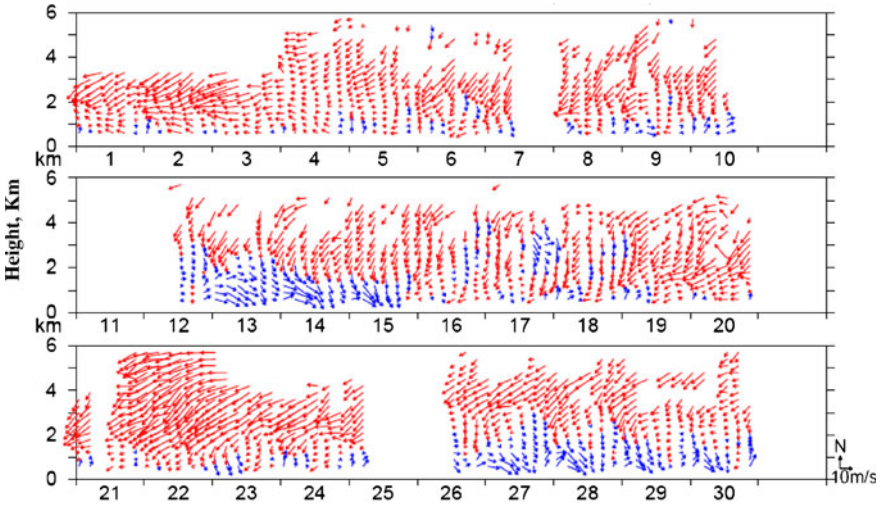

Figure 4. Variation in wind vectors averaged every 4 hours. Vectors are directed upward for a northward (southerly) component, and towards the right for eastward (westerly).

of substantially higher ozone during late evening or night-time, which is discussed in detail in section 3.2.3. LAWP measured horizontal winds averaged for four hours are shown as wind vectors in figure 4. There are some measurement gaps on 7, 11, 12, 25 and 26 April. The wind patterns are clearly dominated by the diurnal thermal regime. A northeasterly stable wind regime could be noticed (figure 4) above 1500 m during the observations. The daytime winds were typically 7 to 10 m/s. Night-time winds were weaker (1–2 m/s) and were from the south or southwest.

Daily variations in the boundary layer height and ozone mixing ratios show a reasonable agreement (figure 5). Average ozone mixing ratios during daytime (1200–1500 hr) and night-time (0000–0003 hr) are also found to be displaying similar variations (figure 5). It has been shown previously that ozone variability is large during spring (Naja and Lal 2002) and standard deviation is estimated to be 16.4 ppbv for this month. Daily average wind speed is seen to be varying between 2 and 5 m/s and surface temperature ranges from about 25° to 40°C during April month. There are very few occasions of rainfall in this month.

The boundary layer height and ozone mixing ratios both are seen to be decreasing from 1 to 5 April and from 16 to 20 April. Both are also found to be increasing from 6 to 13 April and from 22 April onwards. Lowest ozone mixing ratios are observed on a rainy day (22 April) when the boundary layer height is also lower (about 1.5 km). Generally, rain associated with the cloudy condition leads to the reduction in solar radiation that

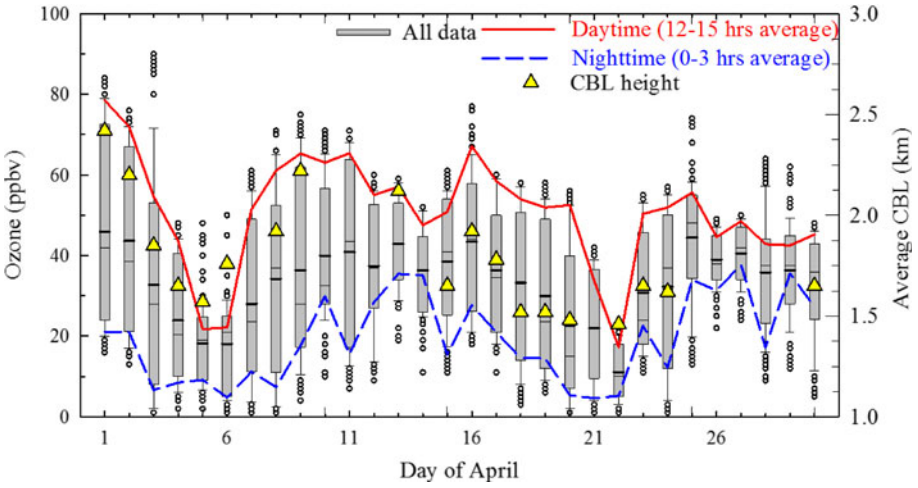

Figure 5. Daily variations in surface ozone and height of the convective boundary layer at Gadanki. Upper and lower sides of box are 75th and 25th percentile and whiskers are 95th and 5th percentiles. Thick and thin lines in the box are mean and median and symbols outside of box are the outliers of 95th and 5th percentiles. Daytime and night-time average ozone data are also shown.

reduces the photochemical ozone production. Additionally, the lower boundary layer height leads to greater ozone loss by surface deposition as well as the lower boundary layer height restricts the mixing of the ozone poor airmass at the surface with the ozone rich airmass at higher heights.

Very high (75–85 ppbv) ozone levels were observed on April 1 and 2, which systematically decreased later (figures 3 and 5). Winds were much stronger and a regime of strong north-easterly or easterly winds dominated during 1–3 April, which subsequently became less dominant (figure 4). Ozone level came down afterward and boundary layer height also followed similar variation. Interestingly, very high ozone levels (about 90 ppbv) are seen during evening on April 3. This will be discussed in section 3.2.3 together with other similar events. Generally, photochemistry is intense during daytime and it is ceased during night-time. There have been occasions when lower ozone levels are observed during the daytime, while substantially higher ozone levels (>70 ppbv) were observed during the night-time. Depending upon this day-to-day variability, events are classified into normal days, rainy day and night-time higher ozone based on the comparison with the monthly average diurnal pattern in ozone. These features are discussed in the following subsections.

3.2.1 *Normal day*

Ozone variations on 4, 9, 17, 18, 19, and 20 April are observed to be a typical normal day variations and are more-or-less similar to the monthly average variation in April (figure 6a). Here, we are using 18 April as representative of normal day variation and is discussed in more detail. It was a clear sunny day and wind speed was lower with mostly northerly or northeasterly (figure 4). In such clear sky conditions, *in situ* ozone production from available precursors takes place during the daytime.

Time-height cross-section of range corrected reflectivity on 18 April (figure 7) shows that a thin enhanced reflectivity layer appeared in the morning at about 400 m and ascended to about 2.5 km in the afternoon. The boundary layer top grew rapidly into the residual layer between 0930 and 1200 hrs and then got prevented from further growth by the strong and sharp capping inversion as shown by the reflectivity plot on this day. At this time, air up to 2.5 km gets convectively well mixed. The mixing of near surface air, which is ozone poor, with that of ozone rich air aloft contributes to the enhancement in the ozone levels near the surface. After about 1300 hrs, the enhanced layer becomes weak gradually. Later, CBL was replaced by a stable or nocturnal boundary layer during night.

Five-day backward trajectory simulation for April 18 (figure 8a) shows that the airmass has been circulating 2–3 days over the continental parts of Indian region. During this residence period of 2–3 days, the airmass got exposed to the local pollution of this region and ozone precursors get accumulated in this airmass, which leads to the daytime ozone production in the favourable meteorological conditions at this site. Thus, normal day ozone mixing ratios at this site are mainly due to the *in situ* photochemistry involving local pollution, convective mixing in a fully evolved boundary layer supplemented with some contribution from the regional transport.

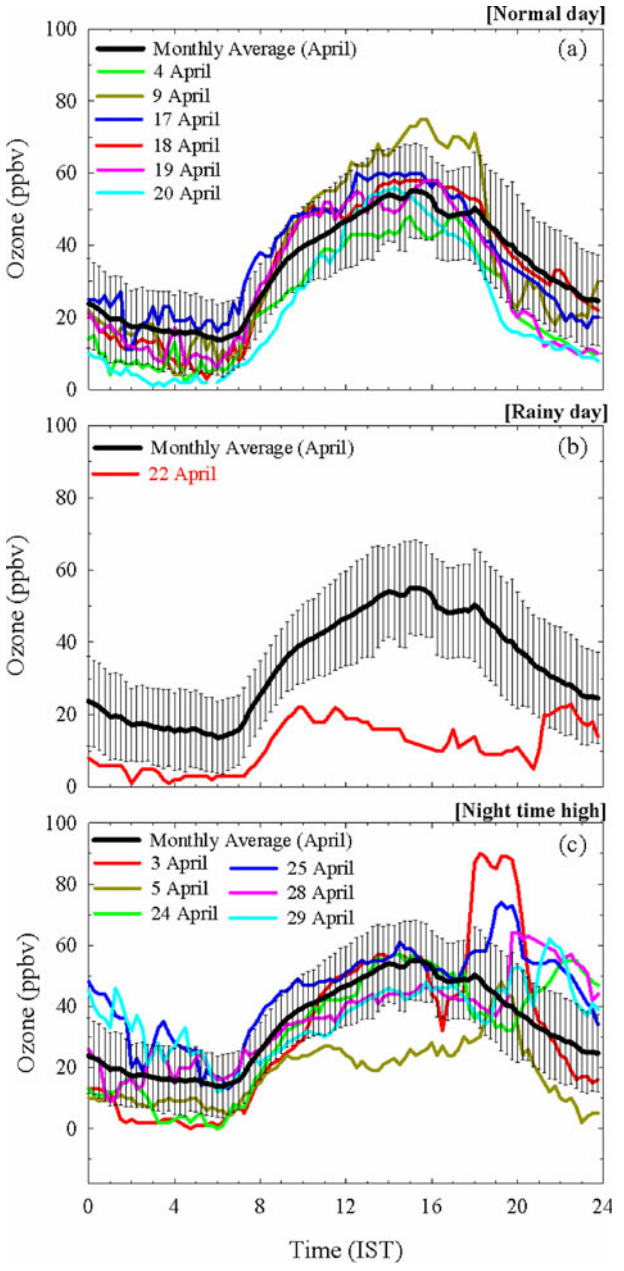

Figure 6. Diurnal variations in surface ozone on (**a**) normal days, (**b**) a rainy day, and (**c**) a night-time higher ozone days in comparison with the monthly average diurnal variation.

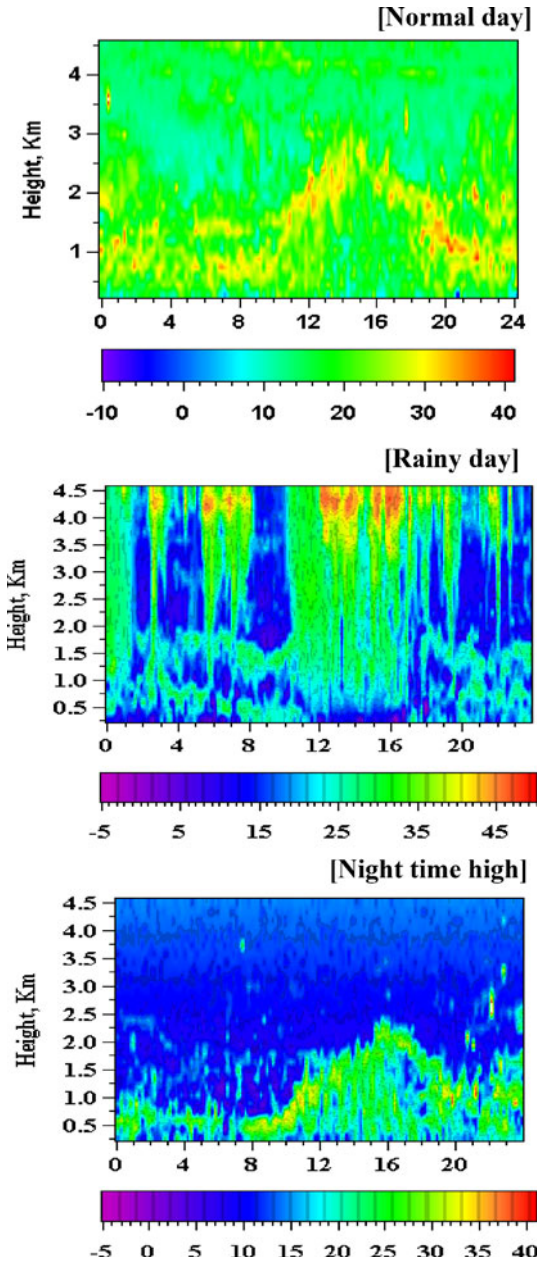

Figure 7. Time-height cross section of range corrected reflectivity averaged over 10 minutes on (**a**) 18 April (a normal day), (**b**) 22 April (a rainy day) and (**c**) 3 April (night-time higher ozone).

3.2.2 *Rainy day*

April 22 was a rainy day and ozone did not show daytime ozone build-up (figure 6b). Daytime and night-time ozone levels are observed to be the lowest on this day for April month. Diurnal amplitude of ozone is only about 12 ppbv, which is only about 30% of average monthly amplitude. The lack of sufficient solar radiation in the presence of clouds and washout of precursor gases during rainy days result in reduced daytime photochemical ozone production.

In a clear contrast with the normal day, wind speeds are observed to be quite higher (more than 20 m/s at higher heights) on this day and the winds are mostly from east. Also, airmass history seen from 5-day backward trajectory clearly shows that the airmass has mostly resided over the Bay of Bengal (4–5 days) before reaching to the observation site and it has not circulated over the continental regions of India for long-enough time to get exposed to the local pollution from this region (figure 8b). Additionally, due to rainfall, precursor gases were also washed out from the atmosphere.

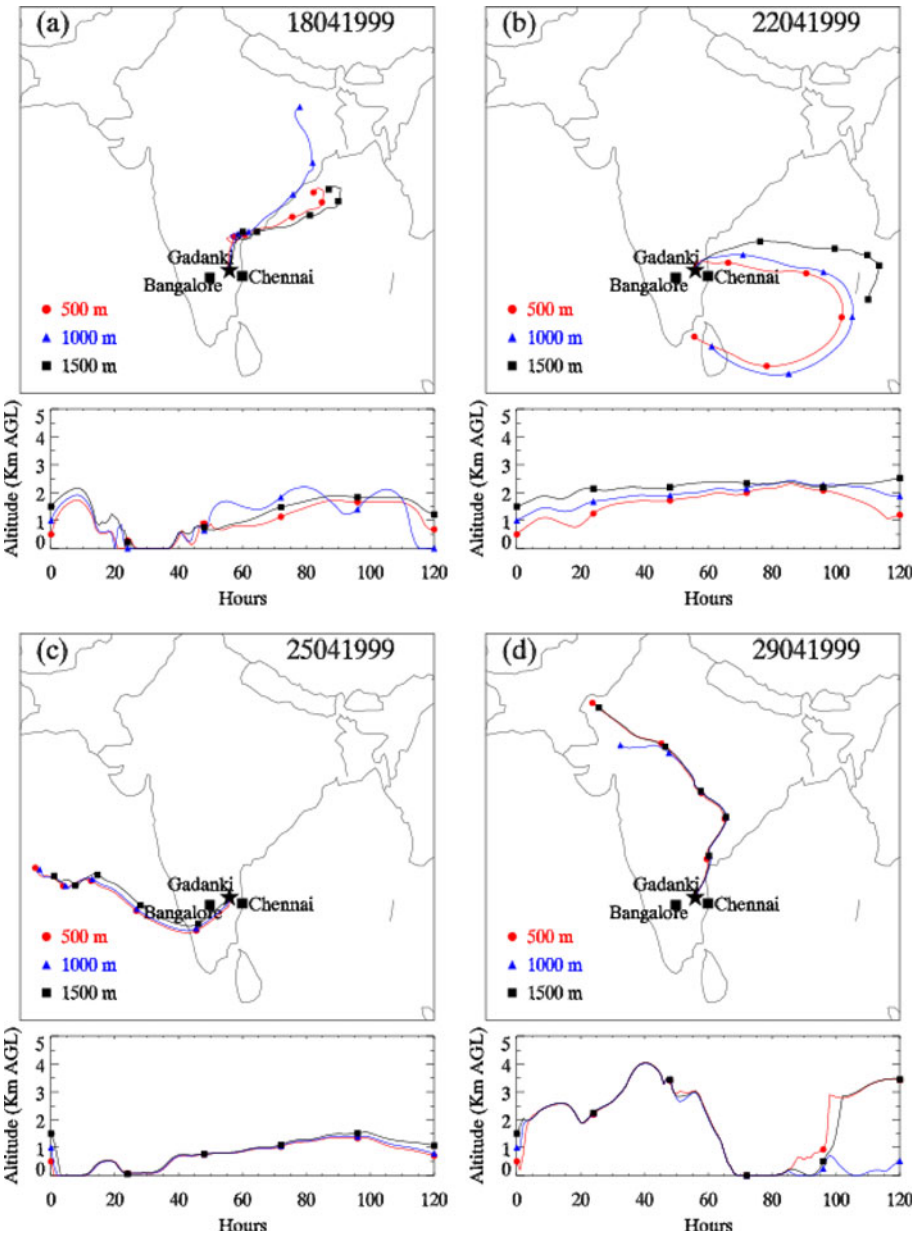

Figure 8. Five days backward trajectories on (**a**) a normal day (April 18), (**b**) a rainy day (April 22), (**c**) night-time high ozone days (April 25), and (**d**) (April 29).

Thus, presence of relatively cleaner airmass along with the cloudy and rainy weather conditions inhibited photochemistry to play significant role on this day.

In such cloudy/rainy conditions, boundary layer also could not evolve much and height of CBL on this day is observed to be the lowest (1.5 km) of this month following similar pattern as that of ozone levels. Lower CBL height prevented the mixing of ozone poor air at the surface with ozone rich air present at higher altitudes. Thus, weaker photochemistry, along with the suppressed convective mixing seems to be the main reason for the observed (lowest) ozone mixing ratios on this day. From the next day (April 23), ozone mixing ratios started increasing and attained the normal levels from 25 April onwards. CBL height has also shown some tendency to increase after 22 April.

3.2.3 *Intrusion of higher ozone in the night-time*

Apart from the normal and rainy days, few days (3, 5, 24, 25, 28 and 29 April) have shown a dramatic increase in ozone levels during late evening and night hours (figure 6c). Since sufficient solar radiation is not available during these evening/night hours, the photochemical ozone production is minimal during these hours and the only possibility

for such higher ozone appears to be the direct transport of ozone rich air to the observation site.

Generally, winds are easterly in the late evening during these days (figure 4). As an example of such events, range corrected reflectivity on April 3 is shown in figure 7(c) and it is observed to be higher (about 35) during 1800–2000 hr. Average CBL height is about 1850 m and vertical velocity show a regime of very strong updraft (1–2.5 m/s) from 1800 hr onward that last up to about 2000 hr. Therefore, based on this updraft event at the present observation site, it is presumed that there might be uplifting of ozone rich air from the surrounding region and reached to the observation site, which led to show rapid enhancement in ozone up to about 90 ppbv during late evening hours (figure 6c).

Similarly, ozone mixing ratios are observed to increase dramatically from 49 to 74 ppbv during 1700 to 2000 hr on April 25 (figure 6c). Unfortunately, boundary layer data are not available on this day but backward trajectory simulated at 1830 hr clearly shows that the air is coming from the southwest and may have influences of the regional pollution during its way to Gadanki (figure 8c). It shows that airmass has been residing

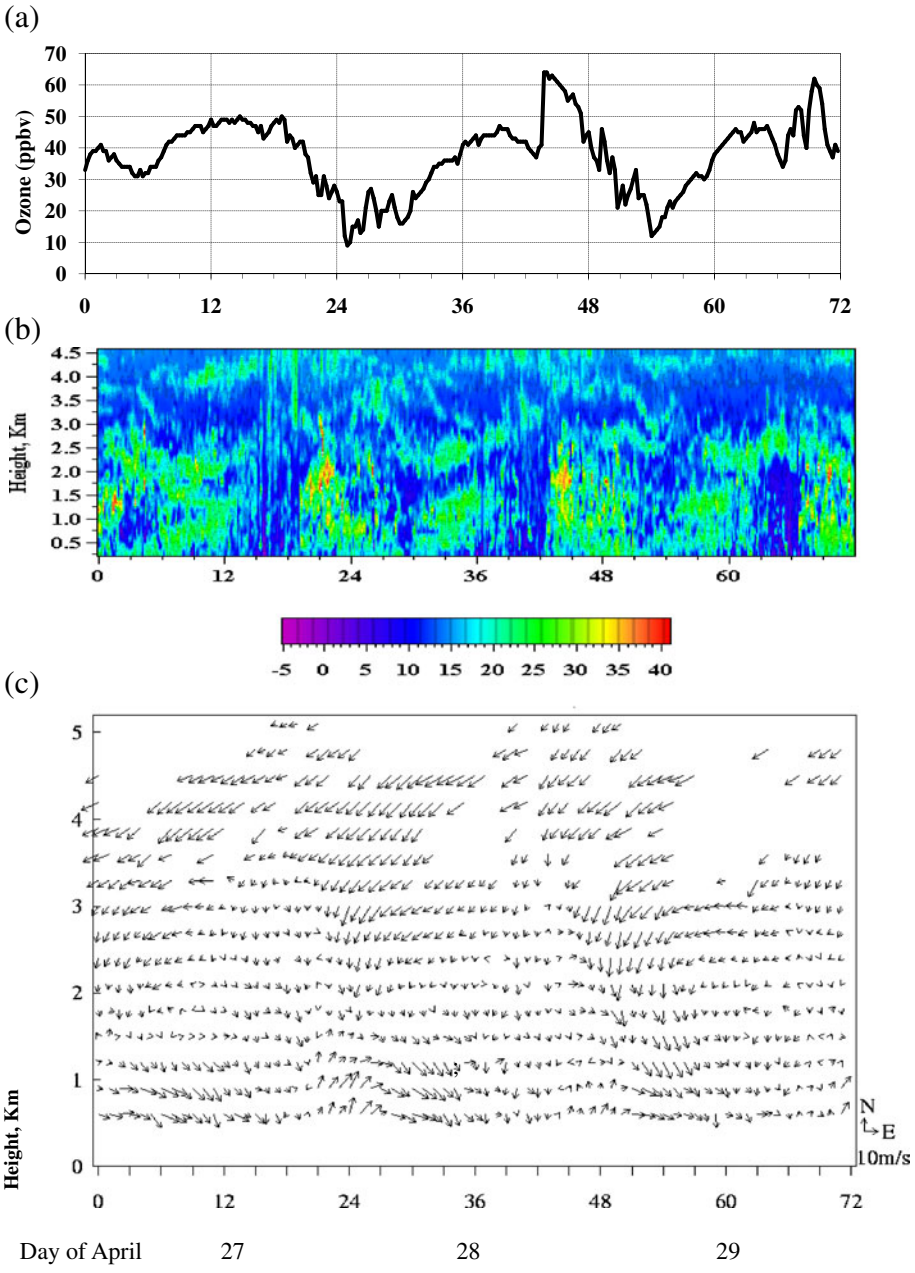

Figure 9. (**a**) Diurnal variation in surface ozone during April 27–29, (**b**) height cross-section of the reflectivity (SNR), (**c**) zonal-meridional winds observed during 27–29 April.

close to Bangalore city for about 1 day and has lifted-up from close to the surface. Also, mountains of varying altitudes are located in the north and northeast (figure 1), which supports that ozone rich air would have been trapped that is advected from the southwest. This air would take a few hours to reach to Gadanki, hence the effect of the advection of ozone rich air is observed only during the late evening hours and onwards. It is to be noted that the airmass has travelled within an altitude of around 1500 m only before reaching to the site, thus the possibility of downward transport of ozone rich air from higher altitudes remains minimal.

Figure 9 shows range corrected reflectivity, evolution in surface ozone and winds during 27, 28 and 29 April. On 28 and 29 April, enhancement in ozone levels are seen during evening hours and wind vectors show a downward motion with northeasterly flow at 3–4 km altitude while the wind becomes northwesterly below 1 km altitude. Reflectivity also shows higher value (35–40) during these periods. Similar to the observed winds, backward trajectory on 28 April (not shown) and 29 April (figure 8d) also show downward transport of airmasses from about 3 to 5 km altitudes. Backward trajectory analysis confirms that the northeasterly airmass are residing over the continental region for all 5 days. Therefore, it is suggested that evening time higher ozone on April 25 is due to uplifting of airmass from southwest polluted center while on April 28 and 29 is due to downward motions from northeastern side.

3.3 *Model simulated ozone variations in normal and cloudy days*

An attempt has been made to examine the influence of photochemistry and planetary boundary layer (PBL) processes on the observed ozone variations. Environmental conditions opted in these simulations are mentioned in table 2. Input background and initial concentrations of CO, CH_4 and NO_x are obtained from measurements at this site (Naja and Lal 2002) while the concentrations of ethane, ethene, propane, propene, *i*-butane, acetylene, *n*-butane, *i*-pentane, isoprene, xylene, and toluene are set to 4, 4, 4, 1.5, 3, 3, 4, 8, 3, 1.3, 1.3 ppbv assuming a typical rural environment. Anthropogenic emissions at this site were obtained from INTEX-B emission inventory. Air temperature and cloud fraction data (MERRA 3-hourly historical data) are used from Goddard Earth Observing System (GEOS) Data Assimilation System. For simulating ozone variation in normal conditions, daytime PBL height is set to 2.5 km, background ozone is set to 42 ppbv, temperature is set to 29°C and cloud free condition is considered. Another run is made for the cloudy condition (cloud fraction 0.21), lower air temperature (27°C) and lower PBL height (1.5 km) as on 5 April. Background ozone level is also set to 36 ppbv. Ozone background levels at 1.5 and 2.5 km over this region have been obtained from ozonesonde observations from Trivandrum.

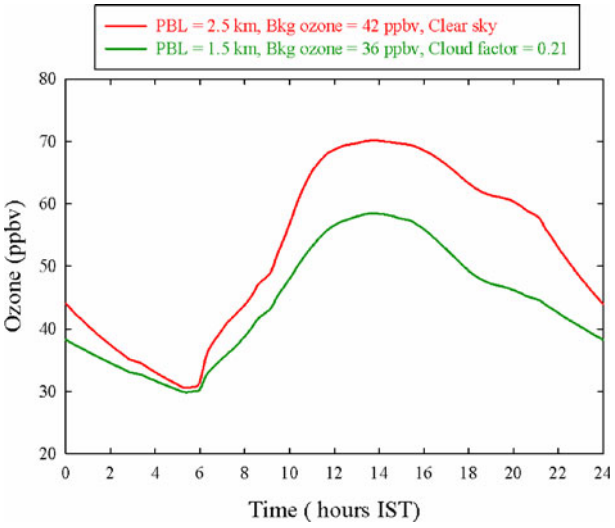

Figure 10. Model simulated ozone variations for normal (clear sky) conditions and cloudy conditions at Gadanki.

The model results for these two cases are shown in figure 10. Here it can be seen that model is able to reproduce the general feature of ozone diurnal

Table 2. *Environmental conditions opted for simulations.*

Temperature	303 K (normal), 298 (cloudy)
Air number density	2.33×10^{19} molecules/cm^3
Relative humidity	50%
Surface albedo	0.10
Parcel elevation	500 m
Overhead O_3 column	260 DU
Aerosol optical depth at 550 nm (vertical, total)	0.235 (for continental aerosol)
Aerosol Angstrom coefficient	1
Aerosol single scattering albedo	0.99

variation at this site. Ozone mixing ratios are significantly higher (∼70 ppbv) during the noon hours on clear sky day. This is mainly due to the more intense photochemistry in the sunny conditions and stronger convective mixing with the ozone rich air aloft. While, in contrast, daytime ozone levels in the event of cloudy condition and lower PBL height are considerably smaller (∼58 ppbv). The reduction of about 17% could be due to combination of PBL processes and cloudy condition. The observations show even higher reduction in the ozone levels when PBL height is lower and has cloudy conditions (22 ppbv on 5 April) in comparison with higher PBL height and sunny day (65 ppbv on 9 April). Both, models as well as observations indicate significant variations in the daytime ozone levels due to changes in boundary layer mixing processes and change in photochemistry induced by cloudy condition. Box model estimated reduction is lesser than that from observations. Here it can be noted that the emissions of ozone precursors have been kept same in both the cases, to isolate the influence of the cloudy condition and the boundary layer processes on ozone levels for unchanged precursors. While ozone precursors due to their shorter chemical lifetime also undergo significant day-to-day variability in their levels. Thus it can be suggested that the difference in model and observations can be associated with the day-to-day variability in the background levels and emissions of various ozone precursors around the measurement site, apart from missing dynamical term in the box model.

4. Summary and conclusions

Simultaneous measurements of surface ozone and the boundary layer evolutions are studied for the first time from a tropical rural site in southern India. The boundary layer and surface ozone have shown day-to-day variability during the measurement period. The boundary layer varied from a minimum height of 1.5 km on a rainy day to a maximum of about 2.5 km during sunny days. Daytime average ozone mixing ratios are observed to follow similar enhancement and reductions as in the convective boundary layer height.

The month of April is dry period/pre-monsoon and also the beginning of summer-hot and very humid in southern India. During this period, maturation of the crops and consequent cessation of evapo-transpiration occur. No significant rain fell (except on 22 April) during April; so soil moisture was probably quite low. It is an ideal situation to form the convective boundary layer at Gadanki region and its depth is one of the fundamental properties that influence ozone variations. Interestingly, events of night-time higher ozone levels are also encountered during the study period. These are shown to be governed mainly by the dynamics, particularly with the uplift and downward motion of airmasses originating from urban cities in the southern India. Therefore, variations in surface ozone mixing ratios are shown to be significantly influenced with the boundary layer dynamics apart from due to the photochemistry. Chemical box model simulations indicate about 17% reduction in the daytime ozone mixing ratios on a cloudy day in comparison with the sunny day. This model estimated reduction is lower than that from the observations. The differences in the model and observations can be due to the day-to-day variability in the levels of ozone precursors. This collocated dataset during one-month experiment could be very useful for a wide range of modelling and analytical studies investigating the role of convective mixing on surface ozone in the tropical Indian region. It is highly desirable to make more such simultaneous observations in different types of environments in India.

Acknowledgements

The authors highly acknowledge Sasha Madronich and coworkers for the development of NCAR-Master Mechanism Box model. The authors are thankful to Kozu T, Nakamura K and Mizutani K for discussions and supporting the Gadanki experiment. Gadanki-LAWP was established under the collaboration between Ministry of Post and Telecommunications (MPT)/Communications Research Laboratory (CRL), Japan and Indian Space Research Organization (ISRO)/NMRF, India. They also like to thank Bhavani Kumar Y and Venkataramani S for regular maintenance of the ozone analyzer. Naja M and Ojha N are thankful to Ram Sagar for his encouragements to this work. Suggestions and comments from the anonymous reviewers are greatly appreciated. The authors gratefully acknowledge the use of HYSPLIT transport and dispersion model (http://www.arl.noaa.gov/ready.php) and Cloud fraction data from Giovanni.

References

Banta R M, Senff C J, White A B, Trainer M, NcNider T T, Valente R J, Mayor S D, Alvarez R J, Mhardesty R M, Parrish D and Fehsenfield F C 1998 Daytime buildup and nighttime transport of urban ozone in the boundary layer during a stagnation episode; *J. Geophys. Res.* **103** 22,519–22,544.

Brasseur G P, Kiehl J T, Muller J F, Schneider T, Granier C, Tie X and Haughlustaine D 1998 Past and future changes

in global tropospheric ozone: Impact on radiative forcing; *Geophys. Res. Lett.* **25** 3807–3810.

Crutzen P J 1995 Ozone in the troposphere, in composition, chemistry, and climate of the atmosphere (ed.) Singh H B, (New York: VanNostrand Reinhold), pp. 349–393.

David L M and Nair P R 2011 Diurnal and seasonal variability of surface ozone and NO_x at a tropical coastal site: Association with mesoscale and synoptic meteorological conditions; *J. Geophys. Res.* **116** D10303, doi: 10.1029/2010JD015076.

Draxler R R and Rolph G D 2011 HYSPLIT (Hybrid Single-Particle Lagrangian Integrated Trajectory) Model access via NOAA ARL READY Website (http://ready.arl.noaa.gov/HYSPLIT.php), NOAA Air Resources Laboratory, Silver Spring, MD.

Fairall C W 1991 The humidity and temperature sensitivity of clear-air radars in the convective boundary layer; *J. Appl. Meteorol.* **30** 1064–1074.

Kleinman L, Lee Y N, Springston S R, Nunnermacker L, Zhou X, Brown R, Hallock K, Klotz P, Leahy D, Lee J H and Newman L 1994 Ozone formation at a rural site in the southeastern United States; *J. Geophys. Res.* **99** 3469–3482.

Krishnan P, Kunhikrishnan P K, Nair S M, Ravindran S, Jain A R and Kozu T 2003 Atmospheric boundary layer observations over Gadanki using lower atmospheric wind profiler: Preliminary results; *Curr. Sci.* **85** 75–79.

Lal S, Naja M and Subbaraya B H 2000 Seasonal variations in surface ozone and its precursors over an urban site in India; *Atmos. Environ.* **34** 2713–2724.

Lelieveld J, Crutzen P J, Ramanathan V, Andreae M O, Brenninkmeijer C A M, Campos T, Cass G R, Dickerson R R, Fischer H, de Gouw J A, Hansel A, Jefferson A, Kley D, de Laat A T J, Lal S, Lawrence M G, Lobert J M, Mayol-Bracero O L, Mitra A P, Novakov T, Oltmans S J, Prather K A, Reiner T, Rodhe H, Scheeren H A, Sikka D and Williams J 2001 The Indian ocean experiment: Widespread air pollution from south and southeast Asia; *Science* **291** 1031–1036.

Madronich S 2006 Chemical evolution of gaseous air pollutants down-wind of tropical megacities: Mexico city case study; *Atmos. Environ.* **40** 6012–6018.

Madronich S and Flocke S 1999 The role of solar radiation in atmospheric chemistry; In: Handbook of Environmental Chemistry (ed.) Boule P (Heidelberg: Springer), pp. 1–26.

Naja M and Lal S 1997 Solar eclipse induced changes in surface ozone at Ahmedabad; *Indian J. Radio Space Phys.* **26** 312–318.

Naja M and Lal S 2002 Surface ozone and precursor gases at Gadanki (13.5°N, 79.2°E), a tropical rural site in India; *J. Geophys. Res.* **107**, doi: 10.1029/2001JD000357.

Naja M, Lal S and Chand D 2003 Diurnal and seasonal variabilities in surface ozone at a high altitude site Mt Abu (24.6°N, 72.7°, 1680 m asl) in India; *Atmos. Environ.* **37** 4205–4215.

Ramachandran, Radhika, Prakash J W J, Gupta K S, Narayanan Nair K and Kunhikrishnan P K 1994 Variability of surface roughness and turbulence intensities at a coastal site in India; *Bound.-Layer Meteorol.* **70** 385–400.

Rao T N and Rao D N 2007 A short review on wind profiler observations of lower and middle atmospheric processes over Gadanki; *Indian J. Radio Space Phys.* **36** 526–542.

Rao S T, Ku Jia-Yeaong, Berman S, Zhang K and Mao H 2003 Summertime characteristics of the atmospheric boundary layer and relationships to ozone levels over the eastern United States; *Pure Appl. Geophys.* **160** 21–55.

Reddy K K, Kumar T R V and Rao D N 1995 Statistical characterization of thermal inversions observed over Tirupati using sodar and microbarograph; *Indian J. Radio Space Phys.* **24** 289–296.

Reddy K K, Kozu T, Ohno Y, Nakamura K, Srinivasulu P, Anandan V K, Jain A R, Rao P B, Ranga Rao R, Viswanthan G and Rao D N 2002 Planetary boundary layer and precipitation studies using lower atmospheric wind profiler over tropical India; *Radio Sci.* **37**, doi: 10.1029/2000RS002538.

Reiner T, Sprung D, Jost C, Gabriel R, Mayol-Bracero O L, Andreae M O, Campos T L and Shetter R E 2001 Chemical characterization of pollution layers over the tropical Indian ocean: Signatures of emissions from biomass and fossil fuel burning; *J. Geophys. Res.* **106** 28,497–28,510.

Rolph G D 2011 Real-time environmental applications and display system (READY) (Website: http://ready.arl.noaa.gov), NOAA Air Resources Laboratory, Silver Spring, MD.

Singal S P, Gera B S and Aggarwal S K 1982 Determination of structure parameter using sodar; *Bound.-Layer Meteorol.* **23** 105.

VanZandt T E, Green J L, Gage K S and Clark W L 1978 Vertical profiles of reflectivity turbulence structure constant: Comparison of observations by the sunset radar with a new theoretical model; *Radio Sci.* **13** 819–829.

White A B, Templeman B D, Angevine W M, Zamora R J, King C W, Russell C A, Banta R M, Brewer W A and Olszyna K J 2002 Regional contrast in morning transitions observed during the 1999 southern oxidants study Nashville/middle Tennessee intensive; *J. Geophy. Res.* **107** 4726, doi: 10.1029/2001JD002036.

Wyngaard J C and LeMone M A 1980 Behaviour of the refractive index structure parameter in the entraining convective boundary layer; *J. Atmos. Sci.* **37** 1573–1585.

Zhang J and Rao S T 1999 The role of vertical mixing in the temporal evolution of ground-level ozone concentrations; *J. Appl. Meteorol.* **38** 1674–1691.

MS received 18 October 2011; revised 27 January 2012; accepted 4 March 2012